WEP Warwick Evans Publishing

International Journal of Natural Resources and Environmental Studies

ISSN: 3006-2012 (Print), ISSN: 3006-0834 (Online) | Volume 8, Number 5, Year 2026
DOI: https://doi.org/10.62051/ijnres.v8n5.01
Journal homepage: https://wepub.org/index.php/IJNRES/index

# Characteristics of Pore Structure in Coal from the Chengzhuang Mining Area

Yilong Chen*

School of Resources and Environment, Henan Polytechnic University, Jiaozuo 454003, China
*Corresponding Author: Yilong Chen (chen4913@126.com)

## ABSTRACT

To investigate the pore structure characteristics and multi-scale distribution of coal in the Chengzhuang mining area, coal samples from the Shanxi Formation were selected for analysis. High-pressure mercury intrusion (MIP), low-temperature nitrogen adsorption (LTNA), and scanning electron microscopy (SEM) were employed to comprehensively characterize pore types, pore size distribution, and pore-throat structure. The results indicate that the pore system in the study area is mainly composed of metamorphic pores and exogenous pores, with relatively poor connectivity. The MIP results show that the pore volume of both samples is dominated by transitional pores, followed by micropores, while mesopores and macropores account for relatively small proportions, suggesting that the pore system is primarily composed of small- to medium-scale pores. The LTNA results reveal that transitional pores contribute significantly to the pore volume, whereas micropores dominate the specific surface area. This indicates that pore volume is mainly controlled by transitional pores, while the specific surface area is primarily governed by micropores.

## KEYWORDS

Pore Structure; High-Pressure Mercury Intrusion; Low-Temperature Nitrogen Adsorption.

## 1. INTRODUCTION

Coalbed methane (CBM) is an important unconventional natural gas resource occurring in coal seams[1]. Formed during long-term coalification processes, CBM is predominantly adsorbed on the internal surfaces of the coal matrix . The effective development and utilization of CBM not only provide a valuable energy resource and contribute to the reduction of greenhouse gas emissions[2], but also play a crucial role in lowering gas concentrations in coal mines, thereby reducing the risk of gas explosions and improving mining safety conditions[3].

Globally, the development of CBM varies significantly due to differences in geological conditions, regulatory frameworks, and technological capabilities [4]. While countries such as Australia and the United States are at the forefront of CBM production, other nations, including China, India, and Indonesia, are actively striving to overcome technical and geological challenges in order to exploit their substantial CBM resources[5,6].

However, despite the considerable progress achieved in CBM exploration and development, the pore structure of coal reservoirs remains highly heterogeneous and complex, which significantly affects gas storage capacity and migration behavior[7-9]. The pore system in coal is generally composed of pores of various scales, ranging from micropores to macropores, each contributing differently to adsorption, diffusion, and seepage processes[10,11]. Therefore, a comprehensive understanding of multi-scale pore structure characteristics is essential for evaluating CBM reservoirs.

## 2. OVERVIEW OF THE STUDY AREA

The Chengzhuang Mine is located approximately 20 km northwest of Jincheng City, spanning Zezhou and Qinshui counties. The industrial site is situated in Shicun Village, Xiacun Town, Zezhou County. The mining area extends approximately 11.607 km in the east-west direction and 10.417 km in the north-south direction. The terrain is characterized by low mountains and hilly landscapes with well-developed gullies. The central area is relatively elevated, while the eastern and western parts are lower. The highest elevation is 1193.22 m at Fangshan Peak in the eastern part, and the lowest elevation is 687.40 m at the Xiachuan River along the southwestern boundary, resulting in a relative elevation difference of 505.82 m.

Loess deposits are widely distributed along the western bank of the Changhe River in the east and the eastern bank of the Qinhe River in the west, while forest vegetation is well developed in the central mountainous area. Villages within the mining area are mainly located along loess gullies or in low-lying areas on hilltops covered by loess. The valley sides are dominated by erosional-depositional landforms, forming floodplains and three levels of river terraces.

The exposed strata in the mining area mainly include the Shangshihezi Formation and the Shiqianfeng Formation, with sporadic outcrops of the Xiashihezi Formation and the Shanxi Formation in the southeastern part. Quaternary deposits are widely distributed along ridges, hills, and both sides of gullies. The coal-bearing strata are primarily the Taiyuan Formation and the Shanxi Formation.

The Taiyuan Formation extends from the base of the K1 quartz sandstone to the base of the K7 sandstone, with a thickness ranging from 67.77 m to 140.62 m and an average thickness of 98.80 m. It is one of the main coal-bearing formations, consisting mainly of dark gray to gray limestone, mudstone, sandy mudstone, siltstone, grayish-white to gray sandstone, and coal seams. It contains 7-16 coal seams, with a coal-bearing coefficient of 7.42%, and the lower coal seams are relatively well developed.

The Shanxi Formation extends from the base of the K7 sandstone to the base of the K8 sandstone and is conformably in contact with the underlying Taiyuan Formation. It is also one of the main coal-bearing formations, composed of grayish-white to gray medium- and fine-grained sandstone, dark gray siltstone, mudstone, and 1-3 coal seams, with a coal-bearing coefficient of 15.05%. Among them, the No. 3 coal seam has an average thickness of 6.24 m and is a stable, mineable seam across the entire study area, representing the only economically recoverable coal seam in this formation.

## 3. SAMPLE COLLECTION AND EXPERIMENTAL METHODS

The samples used in this study were collected from the Chengzhuang and Gaohe mining areas, both from coal seams of the Shanxi Formation. The specific sampling locations are shown in Fig. 1.

**Fig 1** Photos of experimental coal samples

In this study, high-pressure mercury intrusion (MIP), low-temperature nitrogen adsorption (LTNA), and scanning electron microscopy (SEM) were combined to comprehensively characterize the pore structure of coal samples. Based on previous studies, the BBH decimal pore classification scheme was adopted, in which pores are classified according to their size into micropores (0-10 nm), transitional pores (10-100 nm), mesopores (100-1000 nm), and macropores (>1000 nm)[12].

Under this pore size classification system, different experimental methods exhibit distinct characterization ranges and provide different types of information on pore structures. MIP is mainly used to characterize larger-scale pores in coal, with a relatively wide applicable pore size range (>5.5 nm), covering transitional pores, mesopores, and macropores. In contrast, LTNA primarily characterizes micropores and transitional pores (approximately 2-100 nm) and provides quantitative parameters such as specific surface area and pore size distribution. SEM, on the other hand, is mainly used for direct observation of pore morphology and pore types at the microscopic scale, enabling the identification of pore shapes and their connectivity across different scales.

# 4. PORE STRUCTURE CHARACTERISTICS OF COAL

## 4.1. Pore type

The SEM observations of coal samples from the Chengzhuang mining area indicate that the pore types in the coal reservoir are mainly composed of metamorphic pores and exogenous pores, with no well-preserved plant tissue pores observed. Among them, metamorphic pores are predominantly gas pores, which are generally subcircular to elliptical in shape, with smooth pore walls and clear boundaries. These pores exhibit a certain degree of isolation and are typical products formed during hydrocarbon generation and evolution in the coalification process, as shown in Fig. 2(b).

Exogenous pores mainly consist of irregular dissolution pores and intergranular pores formed by tectonic fragmentation. These pores are characterized by irregular shapes and rough boundaries, and local pore wall collapse or particle detachment can be observed, indicating the influence of post-depositional modification processes, as shown in Fig. 2(a, c).

In terms of fracture development, a certain number of microfractures can be observed in the coal samples, which are mainly exogenous fractures formed by tectonic processes. These fractures are generally linear with relatively consistent orientations, smooth fracture surfaces, and small apertures, exhibiting typical characteristics of shear fractures, as shown in Fig. 2(d). Overall, the fractures are limited in number, short in extension, and exhibit poor connectivity.

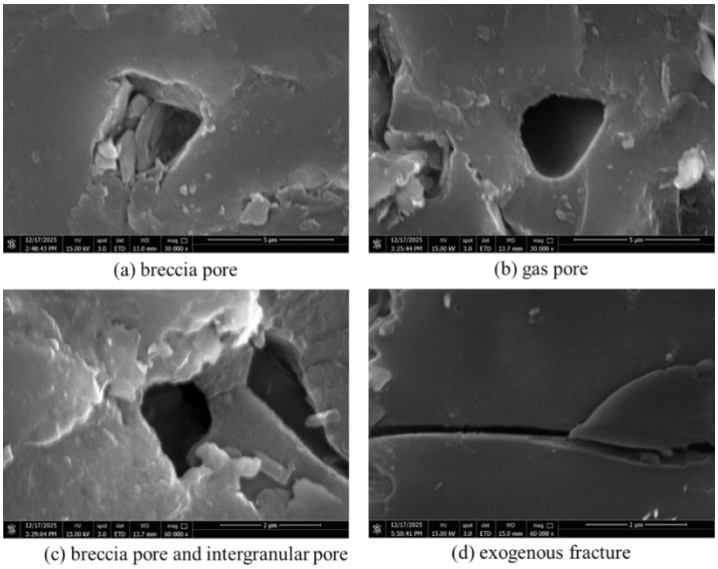


**Fig 2** Scanning electron microscope characteristics of coal samples

## 4.2. Pore Structure Analysis Based on Mercury Intrusion

The results of mercury intrusion porosimetry (MIP) are shown in Table 1. The contributions of different pore size categories to the total pore volume in coal samples from the Chengzhuang mining area exhibit clear patterns. For sample CZ1, the contributions of micropores, transitional pores, mesopores, and macropores are 20.67%, 59.84%, 8.74%, and 10.75%, respectively, whereas for sample CZ2, the corresponding values are 14.54%, 61.95%, 9.71%, and 13.79%.

Overall, both samples are dominated by transitional pores, followed by micropores, while mesopores and macropores account for relatively small proportions. Compared with CZ2, sample CZ1 shows a relatively higher proportion of micropores, whereas CZ2 exhibits slightly higher proportions of transitional pores and macropores. This indicates that there are certain differences in pore structure development between the two samples. However, both samples are generally characterized by a dominance of small- to medium-scale pores, with relatively limited development of large-scale pores.

**Table 1.** Proportion of pore volume for different pore size categories

| Pore size classification | Pore volume proportion (%) | |
|---|---|---|
| | CZ1 | CZ2 |
| Micropores | 20.67% | 14.54% |
| Transitional pores | 59.84% | 61.95% |
| Mesopores | 8.74% | 9.71% |
| Macropores | 10.75% | 13.79% |

The mercury intrusion-extrusion curves are shown in Fig. 3. Both CZ1 and CZ2 samples exhibit pronounced hysteresis loops, indicating the presence of a considerable number of closed or semi-closed pores in the coal matrix, as well as complex pore-throat structures and poor connectivity.

During the mercury intrusion process, the cumulative intrusion volume increases rapidly at the low-pressure stage, suggesting the presence of relatively large pore throats, corresponding to transitional pores and mesopores. As the pressure increases, the growth rate of cumulative intrusion volume gradually decreases, reflecting a transition toward smaller pore sizes and reduced pore throat radii, which makes mercury intrusion more difficult. At the high-pressure stage, the intrusion curve shows a gradual increase again, indicating the presence of a certain amount of smaller pores.

In the mercury extrusion process, the extrusion curves are significantly lower than the intrusion curves and do not overlap, demonstrating a strong hysteresis effect. This indicates that part of the mercury is trapped within the pores and cannot be expelled. This phenomenon is commonly associated with “ink-bottle” type pore structures, characterized by large pore bodies connected by narrow throats, which hinder mercury withdrawal and reflect strong heterogeneity of the pore structure.

A comparison between the two samples shows that the cumulative mercury intrusion volume of CZ1 is significantly higher than that of CZ2, indicating that CZ1 has a larger total pore volume and a higher degree of pore development. Moreover, CZ1 exhibits a larger hysteresis loop area, suggesting a more complex pore-throat structure and a higher proportion of closed or semi-closed pores. In contrast, CZ2 shows a lower mercury intrusion volume and a relatively smoother curve, indicating less developed pore structures.

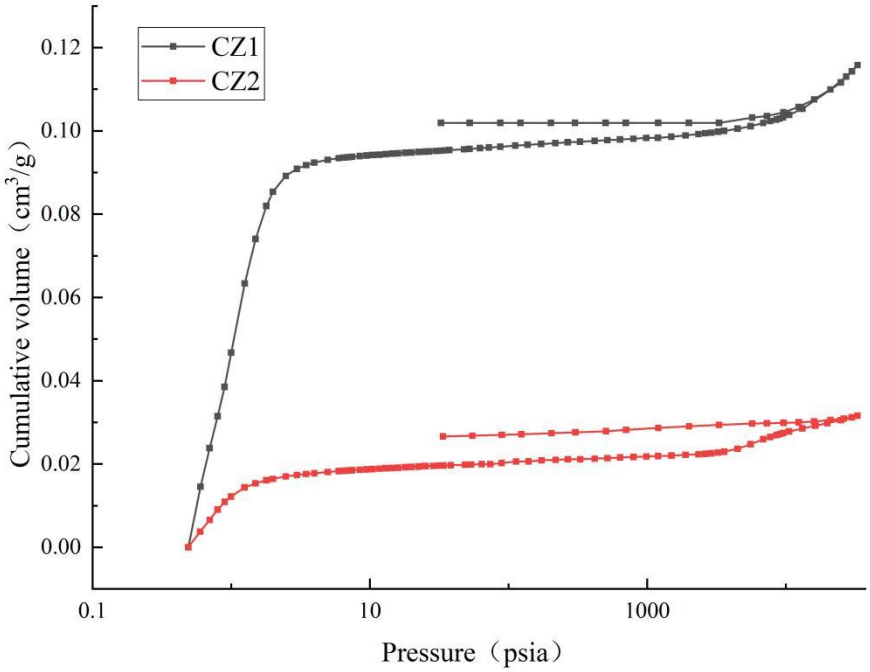


**Fig 3** Mercury entry and exit curves

### 4.3. Pore Structure Analysis Based on Nitrogen Adsorption

The results of low-temperature nitrogen adsorption are presented in Table 2. Significant differences are observed in the pore volume and specific surface area distributions between micropores and transitional pores in coal samples from the Chengzhuang mining area. For sample CZ1, micropores and transitional pores contribute 26.79% and 73.21% to the total pore volume, respectively, whereas for sample CZ2, the corresponding values are 35.16% and 64.84%. These results indicate that transitional pores dominate the pore volume in both samples, although CZ2 exhibits a relatively higher proportion of micropores.

In terms of specific surface area distribution, micropores play a dominant role. For CZ1, micropores and transitional pores contribute 63.50% and 36.50% to the total specific surface area, respectively, while for CZ2, the contributions are 81.92% and 18.08%. It can be seen that although transitional pores dominate the pore volume, micropores make a more significant contribution to the specific surface area. This is particularly evident in CZ2, where the specific surface area is primarily provided by micropores.

**Table 2.** Proportions of pore volume and specific surface area for different pore size categories

| Pore size classification | Pore volume (%) | | Specific surface area (%) | |
|---|---|---|---|---|
| | CZ1 | CZ2 | CZ1 | CZ2 |
| Micropores | 26.79% | 35.16% | 63.50% | 81.92% |
| Transitional pores | 73.21% | 64.84% | 36.50% | 18.08% |

The low-temperature nitrogen adsorption-desorption isotherms are shown in Fig. 4. Both CZ1 and CZ2 samples exhibit similar overall trends. The adsorption isotherms increase rapidly at low relative pressure ($P/P_0 < 0.1$), indicating the presence of a certain amount of micropores, where gas adsorption occurs through rapid pore filling.

At intermediate relative pressures ($0.1 < P/P_0 < 0.8$), the adsorption curves gradually level off, suggesting that transitional pores progressively participate in the adsorption process. At high relative pressures ($P/P_0 > 0.8$), the adsorption capacity increases significantly, and distinct hysteresis loops are observed, indicating the presence of relatively well-developed transitional pores and mesopores

with good openness. The pore structures are relatively complex and exhibit characteristics of "ink-bottle" or slit-shaped pores.

From the morphology of the hysteresis loops, the loops are clearly developed but relatively narrow, suggesting moderate pore connectivity. Some pores are characterized by narrow throats, which hinder gas desorption. This feature is consistent with the pronounced hysteresis observed in the mercury intrusion-extrusion curves, further indicating that the pore-throat structure of the coal is complex and highly heterogeneous.

A comparison between the two samples shows that CZ2 exhibits higher adsorption capacity than CZ1 over the entire relative pressure range, especially at low pressures, indicating that micropores are more developed in CZ2 and that it has a larger specific surface area. This is consistent with the results in Table 2, where micropores contribute a higher proportion (81.92%) to the specific surface area in CZ2. In contrast, CZ1 shows a relatively more pronounced increase in adsorption capacity at high pressures, reflecting a greater contribution from transitional pores, which is consistent with its pore volume distribution characteristics.

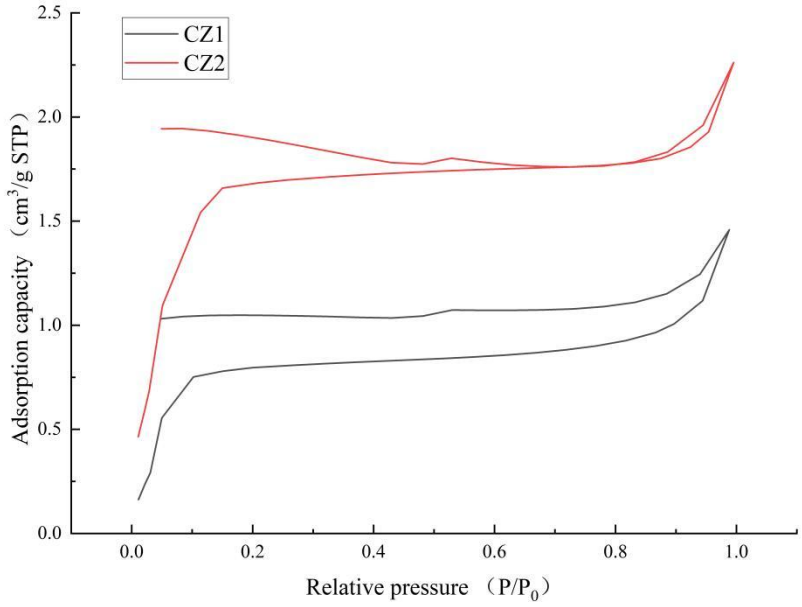


**Fig 4.** Low-temperature nitrogen adsorption-desorption isotherms

## 5. CONCLUSIONS

(1) The pore types of coal samples from the Chengzhuang mining area are mainly composed of metamorphic pores and exogenous pores. Metamorphic pores are primarily gas pores, while exogenous pores are mainly irregular dissolution pores and intergranular pores. No obvious plant tissue pores are observed. Microfractures are poorly developed, dominated by shear fractures with limited extension and poor connectivity.

(2) The mercury intrusion porosimetry results indicate that the pore volume is mainly contributed by transitional pores, followed by micropores, whereas mesopores and macropores account for relatively small proportions. Overall, the pore system is dominated by small- to medium-scale pores. In addition, the mercury intrusion-extrusion curves exhibit pronounced hysteresis, suggesting a complex pore-throat structure.

(3) The low-temperature nitrogen adsorption results show that transitional pores contribute significantly to the pore volume, whereas micropores dominate the specific surface area, reflecting that pore volume is mainly controlled by transitional pores, while the specific surface area is primarily

governed by micropores. The adsorption-desorption isotherms exhibit distinct hysteresis loops, further indicating strong heterogeneity in the pore structure.

## REFERENCES


[1] Guo H, Yu Y, Guo D, et al. Research on physical properties of tectonic coal reservoir and its influence on coalbed methane development: a review[J]. Fuel, 2026, 407.

[2] Ranathunga A S, Perera M S A, Ranjith P G. Deep coal seams as a greener energy source: a review[J]. Journal of Geophysics and Engineering, 2014, 11(6).

[3] Karacan C O, Ruiz F A, Cote M, et al. Coal mine methane: a review of capture and utilization practices with benefits to mining safety and to greenhouse gas reduction[J]. International Journal of Coal Geology, 2011, 86(2-3): 121-156.

[4] Andrews-Speed P, Xu X, Jie D, et al. Deficiencies in China's innovation systems for coal-bed methane development: comparison with the USA[J]. Journal of Science and Technology Policy Management, 2022, ahead-of-print.

[5] Xian B, Liu G, Bi Y, et al. Coalbed methane recovery enhanced by screen pipe completion and jet flow washing of horizontal well double tubular strings[J]. Journal of Natural Gas Science and Engineering, 2022, 99.

[6] Coalbed methane: reserves, production, and future outlook[J]. Future energy, 2020: 97-109.

[7] Li Y, Liu W, Song D, et al. Full-scale pore characteristics in coal and their influence on the adsorption capacity of coalbed methane[J]. Environmental Science and Pollution Research, 2023, 30(28): 72187-72206.

[8] Lu F, Liu C, Zhang X, et al. Study on full-scale pores characterization and heterogeneity of coal based on low-temperature nitrogen adsorption and low-field nuclear magnetic resonance experiments[J]. Scientific Reports, 2024, 14(1): 16910.

[9] Tao S, Pan Z, Chen S, et al. Coal seam porosity and fracture heterogeneity of marcolithotypes in the fanzhuang block, southern qinshui basin, china[J]. Journal of Natural Gas Science and Engineering, 2019, 66: 148-158.

[10] Wang K, Guo L, Xu C, et al. Multiscale characteristics of pore-fracture structures in coal reservoirs and their influence on coalbed methane (CBM) transport: a review[J]. Geoenergy Science and Engineering, 2024, 242: 213181.

[11] Yao Y, Liu D, Che Y, et al. Petrophysical characterization of coals by low-field nuclear magnetic resonance (NMR)[J]. Fuel, 2010, 89(7): 1371-1380.

[12] Guo C, Qin Y, Ma D, et al. Pore structure response of sedimentary cycle in coal-bearing strata and implications for independent superposed coalbed methane systems[J]. Energy Sources, Part A: Recovery, Utilization, and Environmental Effects, 2020: 1-20.